Geophysical Research Letters

RESEARCH LETTER
10.1029/2020GL089504

Quantifying Contributions of Internal Variability and External Forcing to Atlantic Multidecadal Variability Since 1870

Minhua Qin[1], **Aiguo Dai**[2], **and Wenjian Hua**[1]

[1]Key Laboratory of Meteorological Disaster, Ministry of Education (KLME)/Joint International Research Laboratory of Climate and Environment Change (ILCEC)/Collaborative Innovation Center on Forecast and Evaluation of Meteorological Disasters (CIC-FEMD), Nanjing University of Information Science and Technology, Nanjing, China, [2]Department of Atmospheric and Environmental Sciences, University at Albany, State University of New York, Albany, NY, USA

Key Points:
- Observed North Atlantic SST decadal variations resulted mainly from internal variability (IV) since 1870
- Volcanic and anthropogenic aerosols have been in phase with and amplified the IV-induced SST decadal variability since the late 1920s
- Our study helps reconcile the current debate on the role of IV and external forcing in causing Atlantic multidecadal variability

Supporting Information:
- Supporting Information S1

Correspondence to:
A. Dai and W. Hua,
adai@albany.edu;
wenjian@nuist.edu.cn

Citation:
Qin, M., Dai, A., & Hua, W. (2020). Quantifying contributions of internal variability and external forcing to Atlantic multidecadal variability since 1870. *Geophysical Research Letters*, *47*, e2020GL089504. https://doi.org/10.1029/2020GL089504

Received 24 JUN 2020
Accepted 20 OCT 2020
Accepted article online 26 OCT 2020

Abstract Identifying the mechanisms behind the Atlantic Multidecadal Variability (AMV) is crucial for understanding and predicting decadal climate change. However, what is behind the AMV is still debated. A key issue is the relative role of internal variability (IV) and external forcing in causing the AMV. By analyzing observations and a large number of climate model simulations, here we show that IV and volcanic and anthropogenic aerosols all influenced the AMV over the last ~150 years. Although the AMV since 1870 resulted mainly from IV, decadal variations in aerosol forcing happen to be in phase with the IV-induced AMV and thus enlarged its amplitudes, especially since the late 1920s. Our results support the notion that the AMV resulted from both internal climate variability and decadal changes in aerosols but are inconsistent with the conclusion that the recent AMV is mainly a direct response to external forcing.

Plain Language Summary Decadal to multidecadal changes in North Atlantic sea surface temperatures (NASST), commonly known as Atlantic Multidecadal Variability (AMV), influence climate worldwide. The AMV is thought to result from Atlantic ocean circulation and its interaction with the atmosphere, but an ongoing debate is whether external forcing such as decadal variations in aerosols has played a major role in NASST's recent multidecadal variations. Here we show that while internal variability (IV) played a dominant role for the AMV since 1870, decadal variations in volcanic and anthropogenic aerosols acted to enlarge the IV-induced AMV cycles. Our new findings not only reconcile ongoing controversial debate on the role of IV and external forcing in causing the AMV but also provide new convincing evidence on the notion that the recent AMV resulted from both internal climate variability and decadal changes in aerosols.

1. Introduction

The Atlantic multidecadal variability (AMV) or Atlantic Multidecadal Oscillation (AMO) is a 60–80 year basinwide quasi-oscillation in North Atlantic sea surface temperatures (NASST) (Folland et al., 1984; Kerr, 2000; Schlesinger & Ramankutty, 1994). The AMV has significant impacts on multidecadal climate variations over North America (Ruprich-Robert et al., 2018) and Eurasia (O'Reilly et al., 2017; Sutton & Dong, 2012). It also affects Sahelian and South American rainfall (Hua et al., 2019; Knight et al., 2006), Atlantic hurricane activity (Zhang & Delworth, 2006), Arctic sea ice extent (Miles et al., 2014), and even global-mean temperature (Chylek et al., 2014; Dai et al., 2015). While AMV's profound influence on global climate is well documented, the fundamental physical mechanisms and processes underlying the AMV are not fully understood and remain a source of contention (Qin et al., 2020; Sutton et al., 2018; Vecchi et al., 2017).

An ongoing debate is whether external forcing has played a major role in NASST's multidecadal variations during the last 150 years or so. Many modeling studies (Bellomo et al., 2018; Bellucci et al., 2017; Booth et al., 2012; Hua et al., 2019; Murphy et al., 2017; Qin et al., 2020; Watanabe & Tatebe, 2019) suggest that volcanic aerosol (VA) and anthropogenic aerosol (AA) have contributed significantly to the recent AMV. This finding challenges the conventional view that the AMV is an internally generated mode of variability (Zhang et al., 2019). This debate may be partially caused by how we define AMV. A common method is to

detrend NASST either linearly (Enfield et al., 2001) or using observed global-mean SST (GMSST) (Trenberth & Shea, 2006) to remove the long-term warming signal, but such detrending does not accurately estimate and remove the externally forced changes from the observed NASST. This is because the externally forced signal is nonlinear while GMSST contains both internally generated and externally forced variations (Dai et al., 2015; Qin et al., 2020). Thus, the resultant AMV in such detrended NASST is a mix of internally generated and externally forced signals, and it does not provide any attribution information.

Some authors (Steinman et al., 2015) suggested to use AMO to refer to the internal component of NASST's multidecadal variations only, while others (Booth, 2015) suggested to use AMV to depict the total multidecadal variations in NASST from both internal variability (IV) and external forcing to avoid confusion. Such a separation can facilitate the investigation of the different formation mechanisms of the internal and external components, including their different evolutions in the upcoming decades that could have major implications for many regional climates affected by AMV. However, how to properly separate and quantify the internal and external components in NASST still remains a challenge.

Here we analyze SST and other fields from observations and large ensembles of climate model simulations to quantify the contributions from IV and external forcing to the AMV since 1870. The results help define the internal and external components of the AMV and reconcile the current debate on the role of IV and external forcing in causing AMV.

2. Data, Model Simulations, and Methods

2.1. Observational Data and Model Simulations

We used the monthly SST data from 1870–2018 from the Hadley Centre Global Sea Ice and Sea Surface Temperature (HadISST) (Rayner et al., 2003). We analyzed the all-forcing (ALL) historical and RCP4.5 simulations from 38 models participated in Phase 5 of the Coupled Model Inter-comparison Project (CMIP5; Taylor et al., 2012). Additional single-forcing experiments (Table S1. in the supporting information) forced separately by greenhouse gases (GHGs), natural forcing (NAT), AAs, VAs, and solar irradiance (SI) were also used. To ensure the robustness of our results, we also analyzed multimodel ensemble simulations from 27 CMIP6 models (Table S2). We also analyzed the all-forcing 40-member large ensemble of simulations since 1920 by the Community Earth System Model Version 1 (CESM1; Kay et al., 2015). We also used three ensembles of simulations that are identical to the CESM1 all-forcing ensemble, except that one forcing agent is held fixed at the 1920 condition. These include (1) a 20-member CESM1 ensemble with fixed GHGs (hereafter "XGHG"), (2) a 20-member ensemble with fixed industrial aerosols (hereafter "XAER"), and (3) a 15-member ensemble with fixed biomass-burning aerosols (hereafter "XBMB"). The effect from the biomass-burning aerosols is found to be negligible in our analysis, so the XBMB simulations are not discussed further below.

2.2. Methods

Using the GMSST time series from the multimodel ensemble mean (MMM) simulations is a preferred way to define the forced signal, which has the same temporal evolution over all grid boxes because it is determined by the external forcing series (Dai & Bloecker, 2019). To derive the externally forced signal in observations and account for varying bias in model-simulated responses to different forcings, we used a multiple linear regression over 1870–2012 between the GMSST from observations (as the y variable) and the GMSST from CMIP5 or CMIP6 MMM (as the x variables) of single-forcing simulations (i.e., GHG, NAT, and AA, as other external forcings are negligible; see below) to estimate the externally forced global-mean SST ($GMSST_{EX}$) in observations. We then removed this forced signal (i.e., $GMSST_{EX}$) through simple linear regression with local SST series from the observed SSTs at each grid point to produce the residual SST fields that contain primarily internal component. Winton et al. (2020) suggested that a multiple regression method works well to derive different rescaling factors and to remove substantial model biases in response to individual forcings. Following previous studies (Dai et al., 2015), we also used the GMSST from the MMM of all-forcing historical simulations as the first-order estimate of the externally forced signal (see Figure S1). The two methods produced similar results (e.g., $GMSST_{EX}$), although the latter $GMSST_{EX}$ time series shows stronger decadal variations (not shown). After removing the forced components, the residual fields contain primarily the unforced internal variations. The internally generated AMO index is then defined as the low-pass filtered

area-weighted average of the residual SST over the North Atlantic Ocean (80–0°W, 0°–60°N). A Lanczos filter with 19 points and a 13-year cutoff period was used in the low-pass filtering. Statistical significance tests were based on a Student's t test with reduced degree of freedom following Qin et al. (2020).

Following Deser et al. (2020), we subtracted the ensemble mean of XGHG and XAER from the ALL ensemble mean and call these residuals GHG and AER, respectively, which represent the effect from GHG and industrial aerosols. One should note that we removed the long-term linear trend induced by GHG or aerosols to focus on the forced multidecadal variations in NASST. This differs from the linear detrending of observed NASST (Enfield et al., 2001). A simple linear detrending of NASST helps quantify the decadal-multidecadal variations in NASST, but it does not help us attribute either the removed trend or the remaining variations to any particular forcing.

3. Results

3.1. Forced Versus Internal NASST Variations

The observed NASST since 1870 shows multidecadal variations on top of a generally upward trend (Figure 1a). The difference between the observed and forced NASST represents the internally generated component (Figure 1a). The estimated IV shows no obvious trends for the whole period but still accounts for ~37% of the variance in the smoothed NASST series. IV dominates the NASST changes and contributes more than EX to the multidecadal trends in NASST during 1904–2012 (Figure 1b). Furthermore, EX contributes a larger warming in NASST during the recent periods than that before the 1970s (Figure 1b).

Individual external forcing agents may contribute to the NASST decadal variations (Figure 1c). The GHG-forced change is uncorrelated with the IV-induced multidecadal NASST variations during 1870–2012 ($r = -0.04$). In contrast, the NAT and VA forcing simulations show multidecadal variations (Figures 1c and S2, discussed below). The model-simulated NASST response to AA forcing also varies over time, with a large cooling trend during 1944–1974 but small changes during 1904–1944 and 1974–2005 (Figure 1c). The AA-forced interdecadal variations are in phase with the decadal changes in sulfate aerosols from North America and Europe (Figures S2 and S3). Thus, VA and AA may have contributed to the observed decadal NASST variations since 1870.

3.2. Defining the Internal and External Components of AMV

The resultant AMV index is sensitivity to the method used to detrend NASST (Peings et al., 2016; Figure 2a). Recent studies define AMV as the observed NASST signal relative to GMSST and considered it unique to the North Atlantic (Sutton et al., 2018; Yan et al., 2019; Zhang et al., 2019). However, the definition itself does not provide any attribution information. Furthermore, the AMV is a multivariate phenomenon that may require the use of more than SST for its full depiction (Yan et al., 2019; Zhang et al., 2019). To quantify the relative contributions of the internal and external components to the SST-related aspect of the AMV, here we detrended NASST using a physically sound estimate of the externally forced change (see section 2.2). The temporal evolution of this forced GMSST is largely determined by the external radiative forcing and thus is model independent. The regression, which accounts for any systematic model biases, should not alias IV-induced variations into the estimated forced component since the two components are uncorrelated over 1870–2012 ($r = -0.01$; Figure 1a). The residual NASST can be averaged to define an AMO index (Figure 2a, referred to as AMV_{IV}) that represents the IV-induced NASST variations. This index represents the internal component of the AMV, while the E2001 index (also referred to as the total AMV index below) represents the total multidecadal variations in NASST (i.e., due to both IV and external forcing) after removing its long-term linear trend. The difference between the AMV index (i.e., E2001) and our AMV_{IV} index represents the externally forced component in AMV (mainly from GHG, VA, and AA). We call it the AMV_{EX} index (thus, $AMV_{EX} = E2001 - AMV_{IV}$). IV accounts for most (~85%) of the total AMV variations represented by the E2001 index from 1870–2012 (Figure 2a). Our new AMV_{IV} index does not show large amplitudes after 2000, which is different from the widely used AMO indices (Figure 2a).

Figure 2b shows that the multidecadal variations in the EX component (AMV_{EX}) and the multidecadal NASST variations in the GHG-only simulations (after linear detrending, AMV_{GHG}). AMV_{GHG} exhibits a downward trend from 1870–1955 and an upward trend thereafter and shows mostly out-of-phase variations

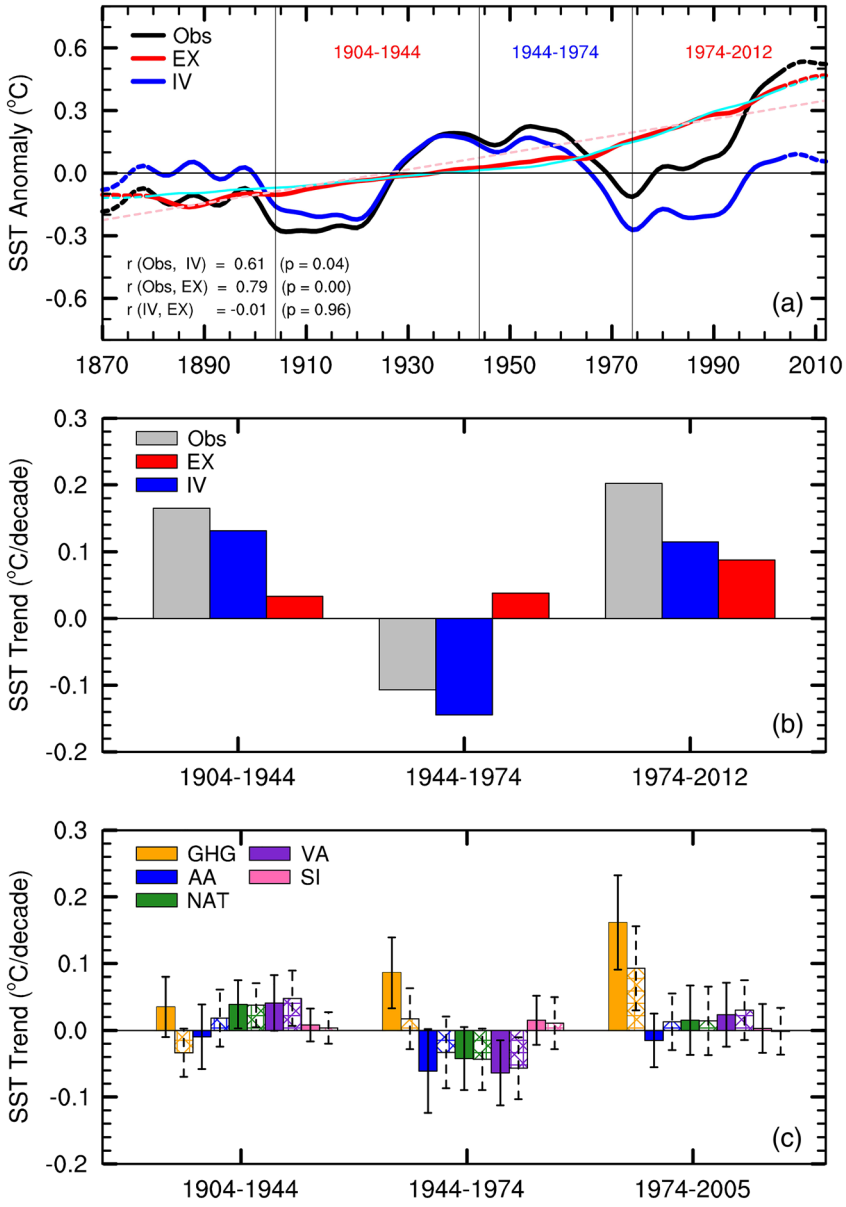

Figure 1. Forced and internal decadal NASST variations. (a) Time series of low-pass filtered, annual-mean SST anomalies (°C, relative to the mean of 1901–1970, the same for all anomalies as it covers roughly one full cycle of the AMV) averaged over the North Atlantic (80–0°W, 0°–60°N) for the observations from 1870–2012 (HadISST1 data set, Obs, black line), estimated externally forced signal (EX, red) and internal variability (IV, dark blue) in the observations. The data near the two ends are derived with mirrored data in the filtering and thus are less reliable; they are marked by the dashed lines. We used the global-mean SST (GMSST) time series from CMIP5 multi-model ensemble mean (MMM) of individual forcing (i.e., GHG, NAT, and AA) simulations to estimate the externally forced signal through multiple linear regression (see section 2.2) and removed it through linear regression from the observed SSTs at each grid point to produce the residual SST fields that contain primarily internal component. The thin red dashed line represents the linear trend for EX. The light blue line shows the low-pass filtered, GMSST from the CMIP5 MMM of the GHG-forcing-only simulations. We rescaled the GMSST from the MMM of the GHG-forcing-only simulations to the observed long-term change at each grid point via linear regression as the estimated observed GHG-forced signal. The thin vertical lines mark the time periods used in (b). The correlation coefficients (r) between the Obs and IV or EX, together with the attained significance level (p), are also shown. (b) North Atlantic SST (NASST) linear trends (°C per decade) from observations (gray), internal variability (blue), and external forcing (red) for three different periods during which the observed NASST starts trending toward opposite directions. Note that some CMIP5 simulations ended in 2005; we included only those simulations extending to 2012 in order to study the recent period. (c) The same as (b) but from the CMIP5 MMM of single-forcing (i.e., GHG, AA, NAT, VA, and SI) simulations. The solid bar denotes the NASST trends without detrending, whereas the hollow bar represents the results with its linear trend over 1870–2005 removed. The error bars denote the standard deviation of inter-model variations.

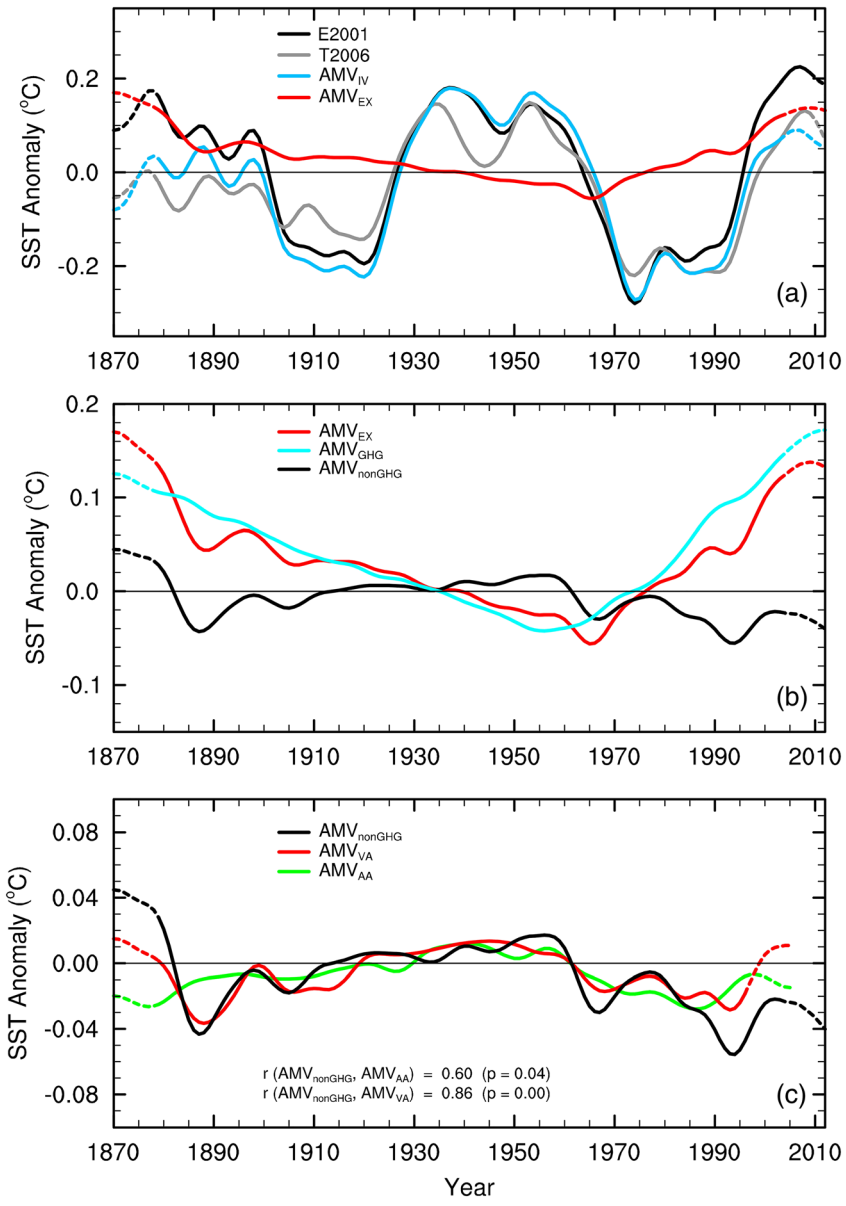

Figure 2. Time series of the AMV indices. (a) The E2001 index (°C, black line) is defined as the local linearly detrended annual-mean SST anomalies (relative to 1901–1970 mean) averaged over the North Atlantic (80–0°W, 0°–60°N) from 1870–2012 as in Enfield et al. (2001). The T2006 index (°C, gray line) is defined as the annual-mean SST anomalies averaged over the North Atlantic but with the global-mean (60°S to 60°N) SST (GMSST) removed as in Trenberth and Shea (2006). The AMV_{IV} index (blue line, the same as the dark blue line in Figure 1a) is defined as the area-weighted average of SST anomalies over the North Atlantic after the component correlated with the GMSST from the CMIP5 MMM of individual forcing (i.e., GHG, NAT, and AA) simulations was removed at each grid point from the observations. The difference between the E2001 index and the AMV_{IV} index represents the externally forced component in AMV (i.e., AMV_{EX}, red line). (b) The AMV_{EX} (red line), which is the sum of the AMV_{GHG} and AMV_{nonGHG}, is the same as the red line in (a). We regressed the local SST anomaly series from observations against the GMSST anomaly series from the MMM of the CMIP5 GHG-forcing-only simulations during 1870–2012 to derive the component associated with the GHG-forcing in observed SST, and then the AMV_{GHG} (light blue line) was derived by averaging this component over the North Atlantic. The AMV_{nonGHG} index (black line) denotes the non-GHG forced variations (i.e., the difference between the AMV_{EX} and AMV_{GHG}). (c) The red (green) line represents the NASST response from the CMIP5 VA (AA) forcing only simulations from 1870–2005 with its linear trend removed. To remove any systematic model biases, we required the sum of the NASST from the MMM of the VA and AA-forcing-only simulations to match the non-GHG forced NASST change from 1870–2005 (i.e., AMV_{nonGHG}) and used this scaling factor to rescale the NASST from the VA and AA-forcing-only simulations before calculating the AMV_{VA} and AMV_{AA} index. All the time series were smoothed with a low-pass filter with a 13-year cutoff period.

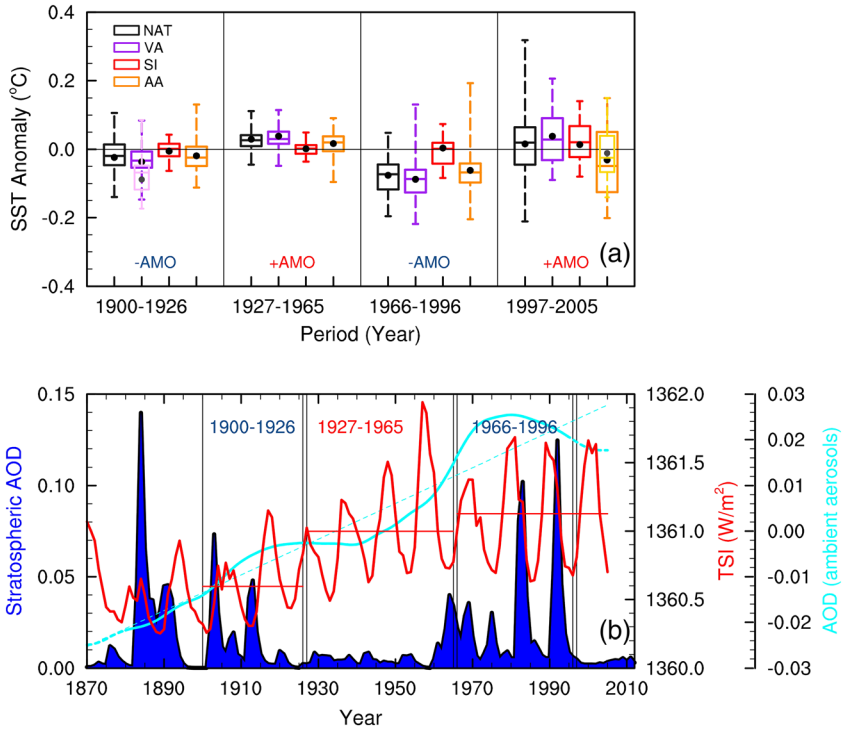

Figure 3. Aerosol-induced multidecadal variations in NASST. (a) The epoch mean of the SST anomalies (°C) during four AMO phase periods from CMIP5 MMM of single forcing (i.e., NAT, VA, SI, and AA) simulations. The multimodel ensemble average is shown by the black dots. The box plots show the distribution of SST anomalies, with the inside line for the median, the box for the 25th and 75th percentile range, and the whiskers for the maximum and minimum values. The bright purple box indicates the epoch mean during 1902–1914 with strong volcanic eruptions. The bright yellow box denotes the epoch mean of SST anomalies during 1996–2012 with AA-forcing model simulations, which extend to 2012. We calculated the SST anomalies from each single forcing simulation with its linear trend from 1870–2005 removed. (b) The Northern Hemispheric mean of stratospheric aerosol optical depth (AOD) at 550 nm as implemented in CMIP5 model simulations for 1870–2012 (black line with blue shading). The light blue line represents the smoothed ambient aerosol optical depth (AOD) at $\lambda = 550$ nm averaged over the North Atlantic from the CMIP5 AA-forcing MMM from 1870–2005 with its linear trend (dashed line). The annual-mean total solar irradiance (TSI, W/m^2, red line) from 1870–2005. Horizontal red lines indicate the epoch mean of the TSI.

uncorrelated with the E2001 ($r = -0.01$) or AMV_{IV} ($r = -0.3$). Thus, GHG forcing mainly increases the NASST anomalies before 1935 and after the 1970s (Figure 2b).

Figure 2c further decomposites the AMV_{nonGHG} into the components forced by VA and AA. Both VA and AA contributed about equally to the non-GHG forced AMV since the 1960s, while the VA forcing accounts for a larger fraction of the non-GHG forced multidecadal variance before 1960 than the AA forcing. The VA-forced component has a higher correlation ($r = 0.86$) than the AA-forced component ($r = 0.60$) with the AMV_{nonGHG} during 1870–2005. The estimated non-GHG forced variation (i.e., AMV_{nonGHG}) corresponds to about ~15% of the amplitude of the AMV_{IV} index, with them roughly in phase since the late 1920s (Figures 2a and 2b). Thus, the VA and AA forcing acts to enlarge the IV-induced AMV cycles. The large AMV amplitudes in the previous indices since ~1995 or 2000 likely resulted from their inclusion of the VA-forced change (i.e., due to the recovering from the 1991 Pinatubo eruption; Maher et al., 2015; Figure S2).

3.3. How Do IV and EX Affect AMV

There is strong evidence that AMOC is a key driver of the AMV (Zhang et al., 2019). The multidecadal variations in the AMOC-related ocean circulation could induce similar variations in NASST, with a strong (weak) AMOC leading to warm (cold) NASST (Figure S4). The well-known horseshoe pattern in the

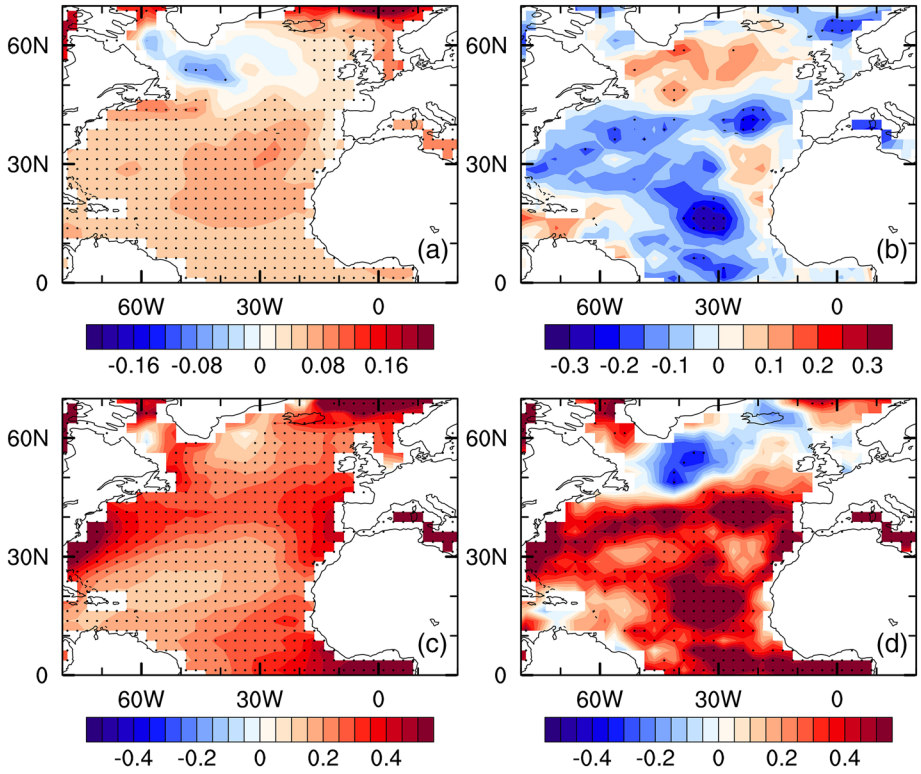

Figure 4. Differences in spatial response between warm and cold phases. AMV warm-minus-cold phase composite differences over the North Atlantic in annual-mean anomalies for (a) sea surface temperatures (SST, °C), (b) total cloud fraction (%), and (c, d) net surface shortwave radiation (W m^{-2}, positive downward) for (c) clear-sky and (d) all-sky conditions from the CMIP5 AA-only simulations. The warm phase periods include 1927–1965 and 1997–2005, and the cold phase periods include 1900–1926 and 1966–1996 based on the IV-induced AMV index (blue line in Figure 2a). The linear trend from 1870–2005 in the AA-only simulations was removed before calculating the anomalies. The stippling indicates that the anomalies are statistically significant at the 5% level based on a Student's *t* test. The results are qualitatively similar when we only use models that include aerosols' indirect effects.

observed NASST is largely caused by IV (e.g., AMOC; Kim et al., 2018), as the IV- and AMOC-induced SST anomaly patterns roughly match the observed SST change patterns (Figures S4 and S5).

How do the aerosols cause the multidecadal NASST variations? Figure 3 shows that large volcanic eruptions during the AMV negative phases (1900–1926 and 1966–1996) cool NASST and thus enhance the IV-induced negative AMV amplitude, while low VA loadings during the two warm phases (1927–1965 and 1997–2005) lead to small impacts on NASST. Thus, VAs affect the AMV mainly by enhancing its amplitude during the cold phases of the IV-induced AMV cycles, as the volcanic eruptions happen to be more frequent during the cold phases. The NASST response to the total solar irradiance (TSI) changes is weak (Figure 3a), as TSI varies quasi-periodically with small amplitudes on an 11-year cycle (Figure 3b) and is uncorrelated with the AMV cycles.

Given the large uncertainties in model simulations of AA's effects (Hua et al., 2018; Sato et al., 2018; Zhang et al., 2013), we analyzed all the available CMIP5 and CMIP6 AA simulations. The multidecadal variations in the AA forcing is roughly in phase with the IV-induced AMV cycles (Figure 3); thus, the NASST response to the AA forcing is positively correlated with and enlarge the IV-induced AMV variations ($r = 0.6$, $p < 0.05$) based on CMIP5 simulations. This is also true for CMIP6 AA forcing only and CESM1 AER simulations ($r > 0.6$, $p < 0.05$).

The positive (negative) decadal anomalies in aerosol loadings roughly correspond to the AMV cold (warm) periods (after linear detrending; Figure 3b). Under the decadal low aerosol loadings over the North Atlantic, net surface shortwave radiation increases under both clear- and all-sky conditions (Figures 4c

and 4d), likely due to AA's direct and indirect effects and water vapor and other feedbacks (Bellucci et al., 2017; Booth et al., 2012). The NASST is strongly correlated spatially with the net surface shortwave radiation in the all-forcing ($r = 0.88$) and AA-forcing-only ($r = 0.7$) simulations, but the correlation is relatively weaker ($r = 0.58$) in the simulations with AA fixed to the preindustrial level (Figure S6). These results indicate that decadal variations in AA forcing since the late 19th century have been roughly in phase with IV-induced AMV and significantly enhanced the AMV mainly through AA's impacts on surface solar heating over the North Atlantic (Figures 4c, 4d, S6c, and S6d). Note that the regional responses of surface solar radiation vary between the CMIP5 and CMIP6 models (Figures 4 and S6). For example, the shortwave radiation response is relatively weak over the tropical North Atlantic in the CMIP6 models (Figure S6c), which is primarily due to small changes in aerosol loadings over the region in CMIP6 (figures not shown).

Interestingly, the responses of SST and surface net shortwave radiations to the AA forcing are weak over the inner subpolar North Atlantic south of Greenland (Figures 4a and S6d). This suggests that other processes may have played a big role in that region. We further examined the responses to AA forcing in North Atlantic SST, wind stress, surface heat flux, and ocean circulations (i.e., AMOC) using the CESM1 AER ensemble of simulations (Figure S7). Increasing (decreasing) aerosols lead to stronger (weaker) AMOC, colder (warming) SST over most North Atlantic, but warmer (colder) SST over the inner subpolar North Atlantic, which leads to higher (lower) surface (sensible plus latent) heat flux in the subpolar region. Note that as the warm and salty subtropical water enters the subpolar region, it loses heat to the air and cools down with increased density, leading to the formation of the North Atlantic Deep Water. Menary et al. (2013) has identified the key role of subpolar North Atlantic sea surface salinity (SSS) in AMOC's response to aerosol changes. A strengthened AMOC in response to increased aerosols is linked to atmospheric circulation changes (Figures S7a and S7b) and an increase in salt advection by the overturning circulation (Menary et al., 2013). The aerosols' cooling effect dominates over the warming effect of the strengthened AMOC in the North Atlantic, except for the inner subpolar region with warm SST anomalies (Figure S7). Similar to the responses to AA forcing, the lack of warming or even with a weak cooling over the midlatitude North Atlantic under increasing GHGs (Figure S8) has been referred to as the North Atlantic warming hole, which has been attributed to surface wind and ocean current changes (Chemke et al., 2020).

4. Conclusions and Discussion

In order to separate and quantify the internally generated and externally forced components in the multidecadal variations in NASST (i.e., AMV), we have analyzed SST and other fields from observations and CMIP5, CMIP6, and CESM1 ensembles of simulations since 1870. We found that the multidecadal variations in NASST (i.e., AMV) has resulted mainly from IV but VA and AA have been in phase with and amplified the IV-induced AMV since the late 1920s through their impacts on surface solar radiation, while the GHG forcing has enhanced the warming in NASST, especially since the 1970s. Furthermore, the recent increasing (decreasing) AA forcing also leads to a strengthened (weakened) AMOC and warm (cold) SST in the inner subpolar North Atlantic while it causes cooling (warming) over the rest of the North Atlantic. Our results are consistent with previous studies (Caesar et al., 2018; Delworth & Dixon, 2006; Menary et al., 2013) suggesting that decreasing AAs or increasing GHGs could force a weakening of AMOC. Moreover, our study extends beyond these previous studies by showing that the recent decadal NASST variations (including SST over the midlatitude North Atlantic) have partly resulted from changes in AAs.

Our finding supports the notion that the recent observed AMV should be viewed as a combination of both IV-induced variations and responses to external forcing (Otterå et al., 2010; Tandon & Kushnir, 2015; Terray, 2012; Ting et al., 2009) but is inconsistent with the conclusion that AMV is mainly a direct response to external forcing (Bellomo et al., 2018; Bellucci et al., 2017; Booth et al., 2012; Murphy et al., 2017; Watanabe & Tatebe, 2019). The latter conclusion is often based on the resemblance of the traditional AMV index (i.e., the linearly detrended, low-pass filtered NASST) between the observations and the externally forced response in model simulations. Our analysis would also lead to such a conclusion if the nonphysical linear detrending is applied to the same data used in Figures 1 and 2 (Figure S9). Thus, the use of the nonphysical linear detrending of the NASST can lead to the incorrect conclusion that AMV is mainly a direct

response to external forcing. Yan et al. (2019) also concluded that the resemblance between linearly detrended observed and CMIP5 forced AMV indices is an artifact of the linear detrending method. Our new AMV_{IV} index can better distinguish and quantify the IV-induced AMV, while the AMV_{EX} and AMV_{nonGHG} indices help quantify the total externally forced and aerosol-forced AMV in observations more accurately than the conventional AMV indices. Their use helps reconcile the current debate on the role of IV and external forcing in causing AMV.

The recent NASST anomalies are not uniformly warm since 2005 as the SST in the Atlantic subpolar gyre region is now as cold as it was in the 1990s (Robson et al., 2016). The recent SST tripole pattern, with cold SST in the Atlantic subpolar gyre and the tropical North Atlantic and warm SST in the subtropical Atlantic, is not representative of the conventional AMV, which shows an overall warming in the North Atlantic. This indicates that the recent NASST changes have more complex causes, including weakened ocean circulation and heat transport and effects from recent increases in GHGs and decreases in AAs (see the supporting information for more discussions).

Our results highlight that the decadal variations in historical VA and AA concentrations over the North Atlantic happen to be in-phase with the IV-induced AMV, leading to an amplification of the AMV by the aerosol forcing. However, we realize that current models have large uncertainties in simulating aerosols' effects. For example, the estimated weak IV-induced SST signal is inconsistent with the recent strengthening of AMOC since 1990 (Chen & Tung, 2018), the strong internally induced AMV-related subpolar North Atlantic SSS changes since 1990 (Yan et al., 2019), and surface turbulent heat flux anomalies during 1990–2005 (Kim et al., 2018). Thus, the CMIP5 and CMIP6 models may overestimate the NASST responses to recent VA and AA. Chylek et al. (2020) suggest that CMIP5 models may overestimate volcanic cooling, especially for boreal winter; such a bias may enlarge our estimated VA effects. The indirect effects of AAs included in many climate models also have been overestimated (Sato et al., 2018; Toll et al., 2019). Current model-simulated NASST and AMOC responses to aerosols may be model dependent. Further efforts to reduce the model deficiencies in simulating aerosols' effects will help improve simulations of the externally forced decadal climate variations.

Data Availability Statement

We thank the climate modeling groups for producing and making available their model output, the Earth System Grid Federation (ESGF) for archiving the data and providing access, and the multiple funding agencies who support CMIP5, CMIP6, and ESGF (https://pcmdi.llnl.gov/CMIP6/). We also acknowledge the CESM Large Ensemble Community Project and supercomputing resources provided by NSF/CISL/Yellowstone (http://www.cesm.ucar.edu/projects/community-projects/LENS/).

Acknowledgments
This study was funded by the National Key R&D Program of China (2016YFA0600702 and 2017YFC1502101) and the National Natural Science Foundation of China (42075022). A. Dai was supported by the U.S. National Science Foundation (Grant Nos. AGS-2015780 and OISE-1743738) and the U.S. National Oceanic and Atmospheric Administration (Award No. NA18OAR4310425). We acknowledge the World Climate Research Programme, which, through its Working Group on Coupled Modelling, coordinated and promoted CMIP5 and CMIP6.

References

Bellomo, K., Murphy, L. N., Cane, M. A., Clement, A. C., & Polvani, L. M. (2018). Historical forcings as main drivers of the Atlantic multidecadal variability in the CESM large ensemble. *Climate Dynamics*, *50*, 3687–3698. https://doi.org/10.1007/s00382-017-3834-3

Bellucci, A., Mariotti, A., & Gualdi, S. (2017). The role of forcings in the twentieth-century North Atlantic multidecadal variability: The 1940–75 North Atlantic cooling case study. *Journal of Climate*, *30*, 7317–7337. https://doi.org/10.1175/JCLI-D-16-0301.1

Booth, B. B. (2015). Why the Pacific is cool. *Science*, *347*, 952. https://doi.org/10.1126/science.aaa4840

Booth, B. B. B., Dunstone, N. J., Halloran, P. R., Andrews, T., & Bellouin, N. (2012). Aerosols implicated as a prime driver of twentieth-century North Atlantic climate variability. *Nature*, *484*, 228–232. https://doi.org/10.1038/nature10946

Caesar, L., Rahmstorf, S., Robinson, A., Feulner, G., & Saba, V. (2018). Observed fingerprint of a weakening Atlantic Ocean overturning circulation. *Nature*, *556*, 191–196. https://doi.org/10.1038/s41586-018-0006-5

Chemke, R., Zanna, L., & Polvani, L. M. (2020). Identifying a human signal in the North Atlantic warming hole. *Nature Communications*, *11*, 1540. https://doi.org/10.1038/s41467-020-15285-x

Chen, X., & Tung, K. (2018). Global surface warming enhanced by weak Atlantic overturning circulation. *Nature*, *559*, 387–391. https://doi.org/10.1038/s41586-018-0320-y

Chylek, P., Folland, C., Klett, J. D., & Dubey, M. K. (2020). CMIP5 climate models overestimate cooling by volcanic aerosols. *Geophysical Research Letters*, *47*, e2020GL087047. https://doi.org/10.1029/2020GL087047

Chylek, P., Klett, J. D., Lesins, G., Dubey, M. K., & Hengartner, N. (2014). The Atlantic Multidecadal Oscillation as a dominant factor of oceanic influence on climate. *Geophysical Research Letters*, *41*, 1689–1697. https://doi.org/10.1002/2014GL059274

Dai, A., & Bloecker, C. E. (2019). Impacts of internal variability on temperature and precipitation trends in large ensemble simulations by two climate models. *Climate Dynamics*, *52*, 289–306. https://doi.org/10.1007/s00382-018-4132-4

Dai, A., Fyfe, J. C., Xie, S.-P., & Dai, X. (2015). Decadal modulation of global surface temperature by internal climate variability. *Nature Climate Change*, *5*, 555–559. https://doi.org/10.1038/nclimate2605

Delworth, T. L., & Dixon, K. W. (2006). Have anthropogenic aerosols delayed a greenhouse gas-induced weakening of the North Atlantic thermohaline circulation? *Geophysical Research Letters*, *33*, L02606. https://doi.org/10.1029/2005GL024980

Deser, C., Phillips, A. S., Simpson, I. R., Rosenbloom, N., Coleman, D., Lehner, F., et al. (2020). Isolating the evolving contributions of anthropogenic aerosols and greenhouse gases: A new CESM1 large ensemble community resource. *Journal of Climate*, *33*, 7835–7858. https://doi.org/10.1175/JCLI-D-20-0123.1

Enfield, D. B., Mestas-Nuñez, A. M., & Trimble, P. J. (2001). The Atlantic Multidecadal Oscillation and its relation to rainfall and river flows in the continental U.S. *Geophysical Research Letters*, *28*, 2077–2080. https://doi.org/10.1029/2000GL012745

Folland, C. K., Parker, D. E., & Kates, F. E. (1984). Worldwide marine temperature fluctuations 1856–1981. *Nature*, *310*, 670–673. https://doi.org/10.1038/310670a0

Hua, W., Dai, A., & Qin, M. (2018). Contributions of internal variability and external forcing to the recent Pacific decadal variations. *Geophysical Research Letters*, *45*, 7084–7092. https://doi.org/10.1029/2018GL079033

Hua, W., Dai, A., Zhou, L., Qin, M., & Chen, H. (2019). An externally-forced decadal rainfall seesaw pattern over the Sahel and Southeast Amazon. *Geophysical Research Letters*, *46*, 923–932. https://doi.org/10.1029/2018GL081406

Kay, J. E., Deser, C., Phillips, A., Mai, A., Hannay, C., Strand, G., et al. (2015). The Community Earth System Model (CESM) large ensemble project: A community resource for studying climate change in the presence of internal climate variability. *Bulletin of the American Meteorological Society*, *96*, 1333–1349. https://doi.org/10.1175/BAMS-D-13-00255.1

Kerr, R. A. (2000). A North Atlantic climate pacemaker for the centuries. *Science*, *288*, 1984–1986. https://doi.org/10.1126/science.288.5473.1984

Kim, W. M., Yeager, S. G., & Danabasoglu, G. (2018). Key role of internal ocean dynamics in Atlantic multidecadal variability during the last half century. *Geophysical Research Letters*, *45*, 13,449–13,457. https://doi.org/10.1029/2018GL080474

Knight, J. R., Folland, C. K., & Scaife, A. A. (2006). Climate impacts of the Atlantic Multidecadal Oscillation. *Geophysical Research Letters*, *33*, L17706. https://doi.org/10.1029/2006GL026242

Maher, N., McGregor, S., England, M. H., & Gupta, A. S. (2015). Effects of volcanism on tropical variability. *Geophysical Research Letters*, *42*, 6024–6033. https://doi.org/10.1002/2015GL064751

Menary, M. B., Roberts, C. D., Palmer, M. D., Halloran, P. R., Jackson, L., Wood, R. A., et al. (2013). Mechanisms of aerosol-forced AMOC variability in a state of the art climate model. *Journal of Geophysical Research: Oceans*, *118*, 2087–2096. https://doi.org/10.1002/jgrc.20178

Miles, M. W., Divine, D. V., Furevik, T., Jansen, E., Moros, M., & Ogilvie, A. E. J. (2014). A signal of persistent Atlantic multidecadal variability in Arctic sea ice. *Geophysical Research Letters*, *41*, 463–469. https://doi.org/10.1002/2013GL058084

Murphy, L. N., Bellomo, K., Cane, M., & Clement, A. (2017). The role of historical forcings in simulating the observed Atlantic Multidecadal Oscillation. *Geophysical Research Letters*, *44*, 2472–2480. https://doi.org/10.1002/2016GL071337

O'Reilly, C. H., Woollings, T., & Zanna, L. (2017). The dynamical influence of the Atlantic Multidecadal Oscillation on continental climate. *Journal of Climate*, *30*, 7213–7230. https://doi.org/10.1175/JCLI-D-16-0345.1

Otterå, O. H., Bentsen, M., Drange, H., & Suo, L. (2010). External forcing as a metronome for Atlantic multidecadal variability. *Nature Geoscience*, *3*, 688–694. https://doi.org/10.1038/ngeo955

Peings, Y., Simpkins, G., & Magnusdottir, G. (2016). Multidecadal fluctuations of the North Atlantic Ocean and feedback on the winter climate in CMIP5 control simulations. *Journal of Geophysical Research: Atmospheres*, *121*, 2571–2592. https://doi.org/10.1002/2015JD024107

Qin, M., Dai, A., & Hua, W. (2020). Aerosol-forced multidecadal variations across all ocean basins in models and observations since 1920. *Science Advances*, *6*, eabb0425. https://doi.org/10.1126/sciadv.abb0425

Rayner, N. A., Parker, D. E., Horton, E. B., Folland, C. K., Alexander, L. V., Rowell, D. P., et al. (2003). Global analyses of sea surface temperature, sea ice, and night marine air temperature since the late nineteenth century. *Journal of Geophysical Research*, *108*, 4407. https://doi.org/10.1029/2002JD002670

Robson, J., Ortega, P., & Sutton, R. (2016). A reversal of climatic trends in the North Atlantic since 2005. *Nature Geoscience*, *9*, 513–517. https://doi.org/10.1038/ngeo2727

Ruprich-Robert, Y., Delworth, T., Msadek, R., Castruccio, F., Yeager, S., & Danabasoglu, G. (2018). Impacts of the Atlantic multidecadal variability on North American summer climate and heat waves. *Journal of Climate*, *31*, 3679–3700. https://doi.org/10.1175/JCLI-D-17-0270.1

Sato, Y., Goto, D., Michibata, T., Suzuki, K., Takemura, T., Tomita, H., & Nakajima, T. (2018). Aerosol effects on cloud water amounts were successfully simulated by a global cloud-system resolving model. *Nature Communications*, *9*, 985. https://doi.org/10.1038/s41467-018-03379-6

Schlesinger, M. E., & Ramankutty, N. (1994). An oscillation in the global climate system of period 65–70 years. *Nature*, *367*, 723–726. https://doi.org/10.1038/367723a0

Steinman, B. A., Mann, M. E., & Miller, S. K. (2015). Atlantic and Pacific multidecadal oscillations and Northern Hemisphere temperatures. *Science*, *347*, 988–991. https://doi.org/10.1126/science.1257856

Sutton, R. T., & Dong, B. (2012). Atlantic Ocean influence on a shift in European climate in the 1990s. *Nature Geoscience*, *5*, 788–792. https://doi.org/10.1038/ngeo1595

Sutton, R. T., McCarthy, G. D., Robson, J., Sinha, B., Archibald, A. T., & Gray, L. J. (2018). Atlantic multidecadal variability and the U. K. ACSIS program. *Bulleting of the American Meteorological Society*, *99*, 415–425. https://doi.org/10.1175/BAMS-D-16-0266.1

Tandon, N., & Kushnir, F. P. J. (2015). Does external forcing interfere with the AMOC's influence on North Atlantic sea surface temperature? *Journal of Climate*, *28*, 6309–6323. https://doi.org/10.1175/JCLI-D-14-00664.1

Taylor, K. E., Stouffer, R. J., & Meehl, G. A. (2012). An overview of CMIP5 and the experiment design. *Bulletin of the American Meteorological Society*, *93*, 485–498. https://doi.org/10.1175/BAMS-D-11-00094.1

Terray, L. (2012). Evidence for multiple drivers of North Atlantic multi-decadal climate variability. *Geophysical Research Letters*, *39*, L19712. https://doi.org/10.1029/2012GL053046

Ting, M., Kushnir, Y., Seager, R., & Li, C. (2009). Forced and internal twentieth-century SST trends in the North Atlantic. *Journal of Climate*, *22*, 1469–1481. https://doi.org/10.1175/2008JCLI2561.1

Toll, V., Christensen, M., Quaas, J., & Bellouin, N. (2019). Weak average liquid-cloud-water response to anthropogenic aerosols. *Nature*, *572*, 51–55. https://doi.org/10.1038/s41586-019-1423-9

Trenberth, K. E., & Shea, D. J. (2006). Atlantic hurricanes and natural variability in 2005. *Geophysical Research Letters*, *33*, L12704. https://doi.org/10.1029/2006GL026894

Vecchi, G. A., Delworth, T. L., & Booth, B. (2017). Climate science: Origins of Atlantic decadal swings. *Nature*, *548*, 284–285. https://doi.org/10.1038/nature23538

Watanabe, M., & Tatebe, H. (2019). Reconciling roles of sulphate aerosol forcing and internal variability in Atlantic multidecadal climate changes. *Climate Dynamics*, *53*, 4651–4665. https://doi.org/10.1007/s00382-019-04811-3

Winton, M., Adcroft, A., Dunne, J. P., Held, I. M., Shevliakova, E., Zhao, M., et al. (2020). Climate sensitivity of GFDL's CM4.0. *Journal of Advances in Modeling Earth Systems*, *12*, e2019MS001838. https://doi.org/10.1029/2019MS001838

Yan, X., Zhang, R., & Knutson, T. R. (2019). A multivariate AMV index and associated discrepancies between observed and CMIP5 externally forced AMV. *Geophysical Research Letters*, *46*, 4421–4431. https://doi.org/10.1029/2019GL082787

Zhang, R., & Delworth, T. L. (2006). Impact of Atlantic Multidecadal Oscillations on India/Sahel rainfall and Atlantic hurricanes. *Geophysical Research Letters*, *33*, L17712. https://doi.org/10.1029/2006GL026267

Zhang, R., Delworth, T. L., Sutton, R., Hodson, D. L. R., Dixon, K. W., Held, I. M., et al. (2013). Have aerosols caused the observed Atlantic multidecadal variability? *Journal of the Atmospheric Sciences*, *70*, 1135–1144. https://doi.org/10.1175/JAS-D-12-0331.1

Zhang, R., Sutton, R., Danabasoglu, G., Kwon, Y.-O., Marsh, R., Yeager, S. G., et al. (2019). A review of the role of the Atlantic Meridional Overturning Circulation in Atlantic Multidecadal Variability and associated climate impacts. *Reviews of Geophysics*, *57*, 316–375. https://doi.org/10.1029/2019RG000644

References From the Supporting Information

Mohino, E., Janicot, S., & Bader, J. (2011). Sahel rainfall and decadal to multi-decadal sea surface temperature variability. *Climate Dynamics*, *37*, 419–440. https://doi.org/10.1007/s00382-010-0867-2

Zhang, R. (2008). Coherent surface-subsurface fingerprint of the Atlantic meridional overturning circulation. *Geophysical Research Letters*, *35*, L20705. https://doi.org/10.1029/2008GL035463

Zhang, R., Delworth, T. L., Rosati, A., Anderson, W. G., Dixon, K. W., Lee, H.-C., & Zeng, F. (2011). Sensitivity of the North Atlantic Ocean Circulation to an abrupt change in the Nordic Sea overflow in a high resolution global coupled climate model. *Journal of Geophysical Research*, *116*, C12024. https://doi.org/10.1029/2011JC007240

Zhang, R., & Vallis, G. K. (2007). The role of bottom vortex stretching on the path of the North Atlantic western boundary current and on the northern recirculation gyre. *Journal of Physical Oceanography*, *37*, 2053–2080. https://doi.org/10.1175/JPO3102.1